Comparison of Poole-Frenkel and Hartke Emission Currents in a Capacitive Micromachined Ultrasonic Transducer (CMUT)

Chukwuebuka Okoro, Sazzadur Chowdhury

Department of Electrical and Computer Engineering

University of Windsor

Windsor, Ontario, Canada

e-mail: okoro3@uwindsor.ca

Abstract— **This study investigates the Poole-Frenkel and 3D Hartke models of electron emission from trap centers in silicon nitride membranes in Capacitive Micromachined Ultrasonic Transducers (CMUTs). The study compared the trap-emitted electron current densities calculated using both models for a CMUT, with a 0.5 micrometer thick silicon nitride structural layer suspended over a 600 nanometer thick vacuum gap. The comparison results demonstrate that the Poole-Frenkel model consistently predicts electronic current densities that exceed the Hartke model predictions by more than 99% for a DC bias voltage range of 11-77 volts. This significant variation in predicted current densities is primarily due to the inclusion of multi-directional emission paths in the Hartke model. In contrast, the Poole-Frenkel model considers emissions only in one direction. The study provides valuable insights into the dielectric charging mechanisms in CMUTs, which can aid in the development of solutions to enhance their reliability.**

Keywords- Quantum Tunneling; Current Density; Hartke; Poole-Frenkel; CMUT; Dielectric Charging.

I. INTRODUCTION

Capacitive Micromachined Ultrasonic Transducers (CMUTs) are reciprocal electrostatic transducers that rely on electrostatic or acoustic vibration of a thin suspended membrane to transmit or receive ultrasound [1]. Experimental results established that the CMUTs offer excellent high-quality high-resolution acoustic data collection capabilities that are not possible with conventional piezoelectric transducers [2]-[3]. As the CMUTs and microelectronic Integrated Circuits (ICs) are made using similar microfabrication processes, the CMUTs can easily be integrated with microelectronic ICs to realize 3D-integrated ultrasound microsystems. Such microsystems, by incorporating both the transducers and processing electronics in a System-In-Package (SIP), can offer superior performance with a better Signal-to-Noise Ratio (SNR).

However, it has been observed that during operation, electrical charge accumulation occurs in the dielectric materials used to realize a CMUT geometry. The phenomenon, known as 'dielectric charging', forces a dynamic shift of the CMUT operating point, causing a drift of the CMUT resonant frequency to affect the vibrational characteristics, output pressure, array operation, and reduced receiving sensitivity [4][5]–[8]. Furthermore, a shift in the electric field due to charge accumulation alters the electromechanical coupling coefficient of a CMUT. In [9]-[11], it was mentioned that the CMUT reliability issue due to the dielectric charging phenomenon must be resolved for mainstream adoption of CMUTs for medical and Non-Destructive Evaluation (NDE) applications.

The primary cause of dielectric charging in CMUTs is widely attributed to trap-assisted [4] and quantum tunneling mechanisms [5][6]. Among these, the Poole-Frenkel (PF) emission and Hartke models provide two distinct theoretical frameworks for describing charge transport in the presence of localized trap states. Silicon nitride, a common dielectric material used to fabricate CMUT membranes, inherently contains structural defects, known as K-center traps [7]. These defects arise during thinfilm deposition processes or from high electric field-induced stress, and they act as charge-trapping sites capable of capturing electrons or holes. Under a strong electric field, these trapped charges can be thermally or field-activated to escape into the conduction band, a process known as field-enhanced thermal emission or the Poole-Frenkel (PF) effect.

In the one-dimensional PF model, the applied electric field reduces the Coulombic potential barrier of the trap, thereby enhancing the likelihood of charge emission along the field direction [8]. However, this model simplifies the potential landscape and does not account for multi-directional emission paths.

The Hartke model extends this concept into three dimensions by averaging the field-lowered barrier over all possible emission angles, thereby offering a more accurate depiction of emission behavior in real materials. This is particularly significant at submicron dielectric thicknesses, which are typical in CMUTs, where charge injection and release occur over a distributed field profile [12].

In this context, this paper compares the values predicted by both the PF and Hartke models in the context of CMUTs. The comparison results can be used for more accurate design of CMUTs to improve their reliability by decreasing the dielectric charging effects.

The remainder of this paper is structured as follows: Section II outlines the theoretical models governing field-induced barrier lowering and electron emission in CMUTs, Section III details the MATLAB-based simulations and provides a comparative analysis of the models, the results and their implications are discussed in Section IV, and finally Section V provides the concluding remarks.

II. CMUT DIELECTRIC CHARGING MODELS

The CMUT is essentially a reciprocal electrostatic transducer that functions as a variable capacitor. Figure 1 shows a typical CMUT geometry, which is constructed to have a dielectric spacer enclosed vacuum or air-filled cavity separating a fixed-edge vibrating membrane and a backplate. In the transmit mode, an AC voltage of desired frequency and amplitude, superposed with a suitable DC bias voltage, is applied across the CMUT electrodes as shown in Figure 1. The resulting time-varying electrostatic attraction force between the CMUT electrodes (top membrane and the fixed backplate) causes the membrane to vibrate and generate ultrasound waves in the medium.

During the receive mode, an incident ultrasound wave forces the membrane to vibrate at the incident wave's frequency. This vibration of the membrane dynamically changes the gap between the membrane and the backplate to affect a change in CMUT capacitance. The capacitance change is converted to an output voltage using a suitable microelectronic circuit and a DC bias. Detailed modeling and operating principles of CMUTs are available in [1][2].

In typical fabrication, full or partial metal-coated silicon or silicon nitride films are used to create the CMUT membranes. Wet, dry or low-temperature silicon dioxide (LTO), and in some designs, the buried oxide layer in silicon-on-insulator (SOI) wafers is used to create the dielectric spacer. Silicon nitride has also been used as dielectric spacers in some cases. Often, an insulating layer on the top of the backplate is used to prevent device damage during membrane collapse.

A. Field-Induced Barrier Lowering

Figure 2 shows the potential energy distribution in a typical field emission system comprised of a metal electrode and an insulator. In Figure 2, E_{FM} is the metal Fermi level, W is the metal work function, χ is the insulator electron affinity, $\vec{E}$ is the applied electric field, d is the insulator thickness, ϕ_B is the potential barrier height, $\Delta\phi_B$ is the electric field induced decrease in potential barrier height, and $\psi(x)$ is the effective potential barrier as a function of distance from the metal surface positioned at the origin (x =0). Following Figure 2, the potential barrier $\psi(x)$ can be expressed as

$$\psi(x) = \begin{cases} 0 & x < 0 \\ V_0 - \chi - q\vec{E}_{diel}x & 0 \le x < d \quad (1) \\ V_0 + q(\vec{E} - \vec{E}_{diel})d - q\vec{E}x & x \ge d \end{cases}$$

where $V_0 = W + E_{FM}$. Due to this barrier lowering as expressed in (1), the charges need a smaller energy to escape from the potential wells (traps) in the insulator. As the trapped charges escape, they contribute to a leakage current and exacerbate dielectric charging, ultimately leading to performance degradation and reliability issues in CMUTs

[7]. A conceptual depiction of this barrier lowering in the context of a CMUT is shown in Figure 3. In Figure 3, the field emission occurs from the top metal electrode surface. As in Figure 2, the interface between the metal and the insulator (Si_3N_4 structural layer of the CMUT membrane) is
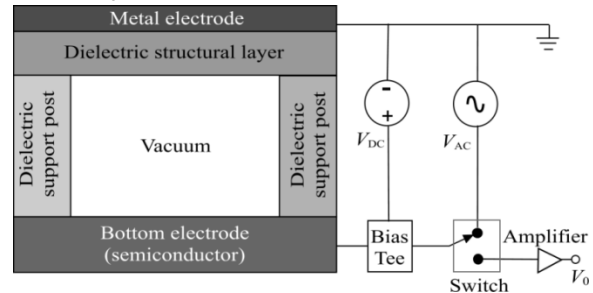

Figure 1.   A typical CMUT geometry in an operational setup.

positioned at $x = 0$ and d depicts the thickness of the Si_3N_4 layer. The metal (typically gold) is characterized by a Fermi level E_{FM} and work function W. As in Figure 2, χ is the electron affinity of the Si_3N_4 layer, and E is the initial longitudinal energy of an electron released from a trap in the nitride layer. As Figure 3 shows, the CMUT bias voltage V_{DC} creates an external electric field $\vec{E}$ across the vacuum gap and an electric field $\vec{E}_{diel}$ across the Si_3N_4 layer, reducing the potential energy barrier in both regions.

B. Poole-Frenkel Emission in CMUTs

The PF emission model assumes that the potential barrier lowering caused by an applied electric field occurs only in one direction [13]. For the CMUT geometry in Figure 3, the PF emission model predicted current density J_{PF} can be calculated from [9][14]:
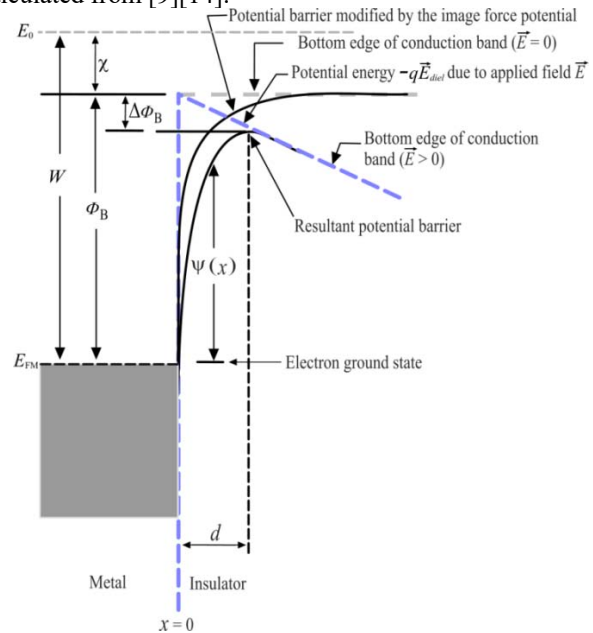

Figure 2.   Schematic diagram of a trap center state of an electron showing the conceptual electron emission due to the applied electric field.

$$\left.\begin{array}{l} J_{PF} = C\vec{E}\exp\left(\dfrac{-\left(\phi-\beta_{pf}\sqrt{\vec{E}}\right)}{kT}\right) \\[2em] \beta_{PF} = \sqrt{\dfrac{q^3}{\pi\varepsilon_0\varepsilon_r}} \end{array}\right\} \quad (2)$$

In (2), the parameter ϕ is the energy level of the charge trap [15]; C is a pre-exponential factor reported as 0.1 A/V-m for Si_3N_4 [16]; β_{PF} is the PF potential barrier lowering coefficient; ε_0 is the permittivity of free space, ε_r is the relative permittivity of the nitride layer; q is the electronic charge; k is the Boltzmann constant and T is the temperature in kelvin.

C. Hartke Emission in CMUTs

Unlike the one-dimensional (1D) PF emission model, the three-dimensional (3D) Hartke emission model incorporates the effect of an applied electric field in a 3D space surrounding the trap centers to characterize the lowering of the potential barrier.

The Hartke model captures this 3D interaction of the electric field with a trap center by introducing angular dependencies where the barrier lowering varies with the angle θ between the direction of the applied field and the emission path, described as $\Delta\phi_{PF}\cos\theta$ [13]. When this barrier lowering relationship is integrated over all possible emission angles, the effective average barrier lowering is obtained. Following the Hartke model [12][13], the emission current density J_H resulting from the electric field $\vec{E}$ associated with the CMUT bias voltage can be
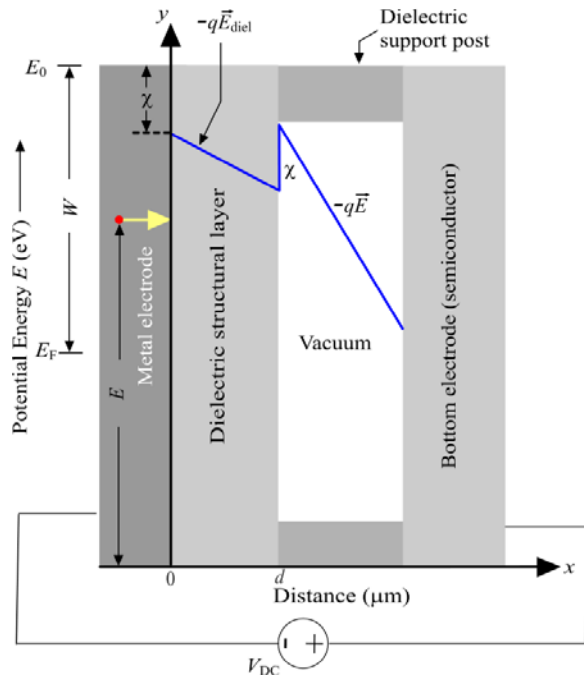

Figure 3. CMUT model showing the triangular barrier lowering due to applied potential energy.

calculated from

$$J_H = \exp\left(\frac{-\phi}{kT}\right)\left(\frac{kT}{\beta\sqrt{E}}\right)^2\left[1+\left(\left(\frac{\beta\sqrt{E}}{kT}\right)-1\right)\exp\left(\frac{\beta\sqrt{E}}{kT}\right)\right]+\frac{1}{2} \quad (3)$$

where the barrier lowering coefficient β and ϕ remains the same as in (2).

It has been observed that this effective average barrier lowering as predicted by the Hartke model is less than the maximum values predicted by the 1D PF emission model [12][13]. This discrepancy, which has its root in the fundamental characterization of the physical phenomenon of charge emission in nitride trap levels, contribute to inaccurate estimation of CMUT leakage currents, which is a major source of dielectric charging in a CMUT.

III. RESULTS

Matlab simulations were conducted to compare the 1D PF model with the 3D Hartke model for a CMUT with specifications and operating conditions as listed in Table 1.

TABLE I.   CMUT SPECIFICATIONS.

Parameters	Dimension	Unit
Top electrode thickness (gold)	0.4	μm
Silicon nitride (Si_3N_4) structural layer thickness	0.5	μm
Vacuum gap thickness	0.6	μm
Bottom electrode thickness (silicon)	0.5	μm
Gap between electrodes	1.1	μm
Temperature	300	K

Figure 4 shows the PF current density J_{PF} as a function of the electric field $\vec{E}$ due to the bias voltage V_{DC} applied to a CMUT with specifications as listed in Table I. As Figure 4 reveals, the PF current density J_{PF} increases rapidly as the effective barrier height decreases with an increasing electric field associated with the 11-77 volts bias voltage range. Similarly, Figure 5 shows the Hartke model predicted
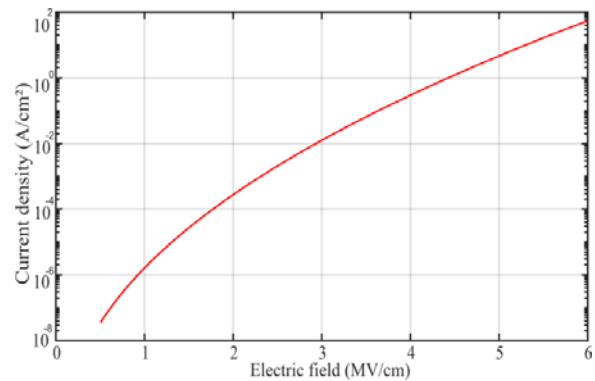

Figure 4. PF model predicted current density due to the trap centers in the CMUT silicon nitride membrane as a function of the lectric field associated with the CMUT bias voltage.
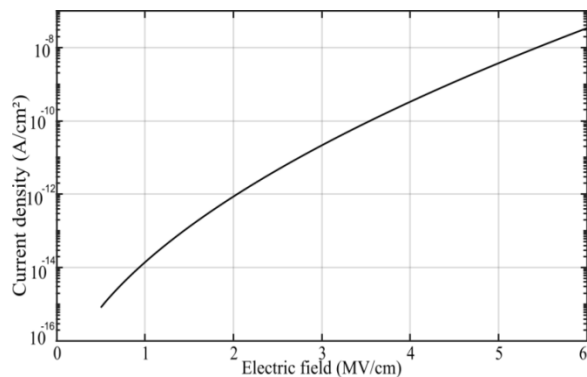
Figure 5.   3D Hartke model predicted current density due to the trap centers in the CMUT silicon nitride membrane as a function of the electric field associated with the CMUT bias voltage.
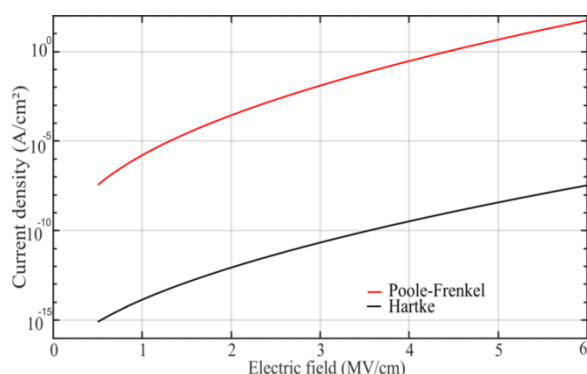

Figure 6.   Current density at 300K for Hartke and PF emission models.

current density J_H as a function of the electric field $\vec{E}$ associated with the same CMUT after applying the same bias voltage. As expected, the Hartke model predicted current density also increases rapidly with an increasing electric field. Figure 6 compares the current densities predicted by both models for the same CMUT geometry subject to the same electric field variations. The percent variations ($\Delta\%$) in the current densities predicted by both the models are tabulated in Table II. As Table II shows, the PF model predicted current density consistently predicts higher current densities compared to the Hartke model by more than 99% for the used bias voltage range.

IV. DISCUSSIONS

Figure 6 and Table II clearly establish that the Hartke model predicted values are order of magnitude smaller than those predicted by the widely used Pool-Frenkel model for the same bias voltage. The reason for this deviation apparently appears to be the directional interaction of the applied electric field with the trap geometry, which is basically a 3D potential well.

The PF model approximates this interaction using a one-directional approach, while the Hartke model considers the 3D nature of the trap. It is therefore safer to conclude that the 3D Hartke model is more realistic for predicting the current density in the silicon nitride membrane of a CMUT.

The trap density in a silicon nitride layer is influenced by

TABLE II.   CURRENT DENSITY COMPARISON.

Bias Voltage (V)	Hartke model current density, J_H (A/cm^2)	Poole-Frenkel model current density J_{PF} (A/cm^2)	$\Delta\%$ $\dfrac{J_{PF} - J_H}{J_{PF}} \times 100$
11	2.689×10^{-12}	1.077×10^{-10}	97.5
22	8.154×10^{-12}	8.771×10^{-10}	99.0
33	2.016×10^{-11}	3.864×10^{-9}	99.47
44	4.425×10^{-11}	1.277×10^{-8}	99.65
55	8.950×10^{-11}	3.555×10^{-8}	99.83
66	1.704×10^{-10}	8.796×10^{-8}	99.80
77	3.099×10^{-10}	1.996×10^{-7}	99.84

the specific composition of silicon and nitrogen within the layer. The parameters of the deposition process, such as plasma-enhanced chemical vapor deposition (PECVD) or low-pressure chemical vapor deposition (LPCVD), greatly influence the composition of the deposited materials in a thin film. It is worth examining the electron trap current densities as a function of both silicon and nitrogen composition in the silicon nitride layer. To carry out this investigation, three different layers of silicon nitride were utilized, each with varying compositions of silicon and nitrogen as listed in Table III [17]. Table III illustrates that there is a direct relationship between the nitrogen content in silicon nitride and the energy trap depth. As the nitrogen content increases, the energy trap depth also increases. Figure 7 shows the corresponding electron current densities, calculated using the Hartke model, plotted as a function of the applied electric field. Figure 7 illustrates that among the 3 investigated silicon nitride layers, the one with the lowest nitrogen concentration (and therefore the lowest energy trap depth of 0.56 eV) results in the highest emission current density at the same electric field strength.

V. CONCLUSION AND FUTURE WORK

The electron current densities resulting from electron emissions from trap centers in microfabricated silicon nitride membranes of CMUTs were examined using both the 1D PF model and the 3D Hartke model. The investigation revealed that the PF model consistently predicts emission current densities that are more than 99% higher than those predicted by the Hartke model within the bias voltage range of 11-77 volts. To provide context, a theoretical study published in [18] concluded that the 1D PF model consistently predicted a 66% higher emission rate compared to the 3D Hartke model for two plane parallel electrodes separated by a dielectric. Obviously, the PF model overestimates the emission current.

TABLE III.   DIFFERENT SILICON NITRIDE COMPOSITIONS WITH CORRESPONDING TRAP DEPTHS

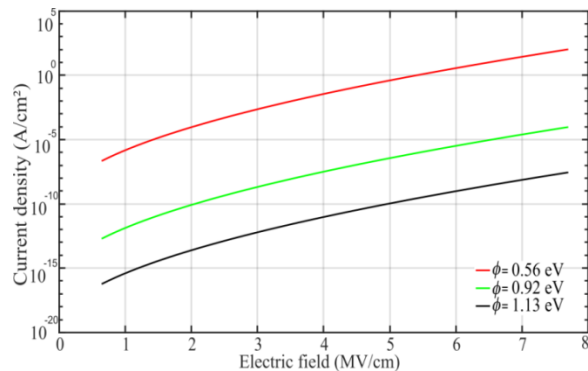| Composition	Trap depth/ionization potential ϕ (eV)
$SiN_{0.75}$	0.56
$SiN_{1.17}$	0.92
$SiN_{1.22}$	1.13

Figure 7.   The Hartke model predicted current densities for three different silicon nitride layers with varying composition of silicon and nitrogen and trap depth energy levels as listed in Table III.

Apparently, this is due to its assumption of a one-dimensional potential barrier lowering. However, the Hartke model, which takes into account the three-dimensional behavior of traps, aligns more closely with actual trap behavior. It can be concluded that, in comparison to the PF model, the Hartke model is a more accurate method for predicting the emission current in 3D microstructures, such as a CMUT that uses a vibrating silicon nitride membrane to transmit or receive ultrasound.

Furthermore, during vibration, the silicon nitride membrane of a CMUT deforms causing distortion of the energy levels of the charge traps located within the membrane. It is thus necessary to evaluate the Hartke model predicted current densities in dynamically vibrating CMUT membranes against experimentally measured values.

REFERENCES

[1]   J. Jayapandian, K. Prabakar, C. Sundar, and B. Raj, "On the Design, Fabrication, and Characterization of cMUT Devices," in Materials and Failures in MEMS and NEMS, 1st ed., A. Tiwari and B. Raj, Eds., Wiley, 2015, pp. 201–218. doi: 10.1002/9781119083887.ch6.

[2]   P. Zhang, G. Fitzpatrick, W. Moussa, and R. Zemp, "CMUTs with improved electrical safety & minimal dielectric surface charging," in Proc. 2010 IEEE International Ultrasonics Symposium, San Diego, CA, USA: IEEE, Oct. 2010, pp. 1881–1885. doi: 10.1109/ULTSYM.2010.5935744.

[3]   N. Tavassolian, "Dielectric charging in capacitive RF MEMS switches with silicon nitride and silicon dioxide," PhD Dissertation, Georgia Institute of Technology, 2011.

[4]   X. Zhang, H. Zhang, and D. Li, "Design of a hexagonal air-coupled capacitive micromachined ultrasonic transducer for air parametric array," Nanotechnology and Precision Engineering, vol. 4, no. 1, p. 013004, Mar. 2021, doi: 10.1063/10.0003504.

[5]   S. Machida, T. Takezaki, T. Kobayashi, H. Tanaka, and T. Nagata, "Highly reliable CMUT cell structure with reduced dielectric charging effect," 2015 IEEE International Ultrasonics Symposium (IUS), Taipei, Taiwan, 2015, pp. 1-4, doi: 10.1109/ULTSYM.2015.0061

[6]   S. O. Kasap, Principles of electronic materials and devices, Fourth edition. New York, NY: McGraw-Hill, 2018.

[7]   X. Yuan, et al, "Initial Observation and Analysis of Dielectric–Charging Effects on RF MEMS Capacitive Switches", in Proc. 2004 IEEE MTT–S International Microwave Symposium Digest, vol. 3, 2004, pp. 1943–1946

[8]   H. Wang, Y. Tong, X. Wang, C. He, and C. Xue, "Experimental investigation of the influence of excitation signal on radiation characteristics of capacitive micromachined ultrasonic transducer," Microsyst Technol, vol. 24, no. 12, pp. 5055–5063, Dec. 2018, doi: 10.1007/s00542-018-4131-8.

[9]   J. Li, Y. Li, and P. Zhang, "Modelling and Analysis of Dielectric Charge of CMUTs," IOP Conf. Ser.: Mater. Sci. Eng., vol. 768, no. 6, p. 062106, Mar. 2020, doi: 10.1088/1757-899X/768/6/062106.

[10]   M. Koutsoureli, D. Birbiliotis, L. Michalas, and G. Papaioannou, "Dielectric charging in MEMS capacitive switches: a persisting reliability issue, available models and assessment methods," in Proc. of 2016 16th Mediterranean Microwave Symposium (MMS), Abu Dhabi, United Arab Emirates: IEEE, Nov. 2016, pp. 1–4. doi: 10.1109/MMS.2016.7803802.

[11]   J. Munir, Q. Ain, and H. Lee, "Reliability issue related to dielectric charging in capacitive micromachined ultrasonic transducers: A review," Microelectronics Reliability, vol. 92, pp. 155–167, Jan. 2019, doi: 10.1016/j.microrel.2018.12.005.

[12]   J. Hartke, "The Three-Dimensional Poole-Frenkel Effect," Journal of Applied Physics, vol. 39, no. 10, pp. 4871–4873, Sep. 1968, doi: 10.1063/1.1655871.

[13]   O. Mitrofanov and M. Manfra, "Poole-Frenkel electron emission from the traps in AlGaN/GaN transistors," Journal of Applied Physics, vol. 95, no. 11, pp. 6414–6419, Jun. 2004, doi: 10.1063/1.1719264.

[14]   V. Kapoor and S. Bibyk, "Energy distribution of electron-trapping centers in low-pressure chemically vapor-deposited Si3N4 films," Thin Solid Films, vol. 78, no. 2, pp. 193–201, 1981, doi: https://doi.org/10.1016/0040-6090(81)90619-2.

[15]   Y. Zhou and P. Zhang, "Theory of field emission from dielectric coated surfaces," Phys. Rev. Research, vol. 2, no. 4, p. 043439, Dec. 2020, doi: 10.1103/PhysRevResearch 2.043439.

[16]   "The Reliability of the Silicon Nitride Dielectric in Capacitive MEMS," Docslib. [Online]. Available: https://docslib.org/doc/505598/the-reliability-of-the-silicon-nitride-dielectric-in-capacitive-mems, Retrieved: Feb., 2025.

[17]   R. Apodaca, "Electrical Characterization of Silicon-Rich Nitride and Silicon Oxynitride Films Deposited by Low-Pressure Chemical Vapor Deposition," Master's Thesis, University of New Mexico. Electrical Engineering, 2005.

[18]   P. Murgatroyd, "Theory of space-charge-limited current enhanced by Frenkel effect," J. Phys. D: Appl. Phys., vol. 3, no. 2, pp. 151–156, Feb. 1970, doi: 10.1088/0022-3727/3/2/30